Bioorganic & Medicinal Chemistry Letters 22 (2012) 1165–1168

Contents lists available at SciVerse ScienceDirect

Bioorganic & Medicinal Chemistry Letters

journal homepage: www.elsevier.com/locate/bmcl

Potent and selective pyrazolo[1,5-*a*]pyrimidine based inhibitors of B-Raf^{V600E} kinase with favorable physicochemical and pharmacokinetic properties

Li Ren [a,*], Ellen R. Laird [a], Alex J. Buckmelter [a], Victoria Dinkel [a], Susan L. Gloor [a], Jonas Grina [a], Brad Newhouse [a], Kevin Rasor [a], Gregg Hastings [a], Stefan N. Gradl [b], Joachim Rudolph [b]

[a] Array BioPharma, Inc., 3200 Walnut Street, Boulder, CO 80301, USA
[b] Genentech, Inc., 1 DNA Way, South San Francisco, CA 94080-4990, USA

ARTICLE INFO

Article history:
Received 29 October 2011
Revised 18 November 2011
Accepted 21 November 2011
Available online 30 November 2011

Keywords:
B-Raf
Kinase
Drug discovery
Cancer

ABSTRACT

Herein we describe a novel series of ATP competitive B-Raf inhibitors based on the pyrazolo[1,5-*a*]pyrimidine scaffold. These inhibitors exhibit both excellent cellular potency and striking B-Raf selectivity. Optimization led to the identification of compound **17**, a potent, selective and orally available agent with improved physicochemical and pharmacokinetic properties.

Activation of the Ras/Raf/MEK/ERK (MAPK) signal transduction cascade leads to cellular proliferation, differentiation, and survival.[1] The Raf family is central to this pathway, and consists of the serine/threonine kinases A-Raf, B-Raf, and C-Raf, which phosphorylate and activate MEK.[1] Mutations in the B-Raf gene may lead to MAPK pathway amplification via constitutive activation of B-Raf, and are present in ~7% of all cancers,[2] with particular frequency in melanoma.[3,4] Over 90% of detected mutations in B-Raf involve a single glutamic acid for valine substitution at residue 600 (V600E),[2] which leads to constitutive kinase activity 500-fold greater than wild-type B-Raf,[5] and correlates with increased malignancy and decreased response to chemotherapy.[6] Small molecule inhibitors of B-Raf^{V600E} represent an attractive strategy for therapeutic intervention in cancers that are induced by this mechanism of pathway activation.[7] Vemurafenib is currently the only approved inhibitor that is selective for B-Raf^{V600E},[8] although three are in clinical trials[9] and others are in preclinical development.[10]

We recently reported the discovery of a series of potent amide-based inhibitors of B-Raf^{V600E}.[11] These compounds, for example **1**, occupy the ATP cleft with a pyrazolopyridine template and form two hydrogen bonds with the –NH and carbonyl of Cys532. The fused bicycle was designed to enhance a π-stacking interaction with the indole of Trp531. The propyl sulfonamide moiety forms several hydrogen bonds with the backbone of the DFG sequence, while the propyl chain occupies a small lipophilic pocket that is enlarged by an outward shift of the αC-helix. Based on an optimal combination of pERK activity (IC_{50} = 19 nM), mouse pharmacokinetic exposure, and tumor growth inhibition activity,[11] **1** was selected as a promising lead for further preclinical evaluation. However, the low solubility of **1** (4 μg/mL at pH 6.5) precluded the use of crystalline suspension formulations in efficacy and toxicology studies, and an amorphous spray-dried dispersion formulation was necessary.[11] While this formulation has been successfully used in the clinic for poorly soluble drugs, issues associated with amorphous dispersion formulation, such as physical form stability and high pill burden, pose potential challenges for development.[12]

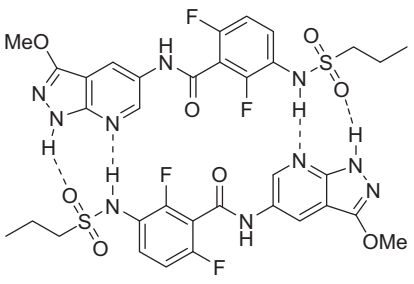

1

Figure 1. Schematic of the head-to-tail dimer formation of **1**, as observed in a single crystal X-ray.

* Corresponding author.
E-mail address: li.ren@arraybiopharma.com (L. Ren).

0960-894X/$ - see front matter © 2011 Elsevier Ltd. All rights reserved.
doi:10.1016/j.bmcl.2011.11.092

Thus, a potent and selective B-Raf^{V600E} inhibitor with improved aqueous solubility would be highly desirable.

A single crystal X-ray structure of **1** revealed a head-to-tail dimer formation in the crystal lattice, as illustrated schematically in Figure 1. Four intermolecular hydrogen bonds between the pyrazolopyridine hinge binding template and the propyl sulfonamide tail contribute to the dimer formation, and result in high melting point (mp = 229 °C) and high crystal lattice energy.[13]

To address the liabilities of lead compound **1**, we opted to improve solubility by disrupting the propensity for dimer formation (crystal packing). Wishing to retain the propyl sulfonamide moiety, which is a key feature for the DFG-in/C-helix shifted binding mode, we focused on exploring alternative hinge binding templates. Since dual hinge binding templates have the potential to form head-to-tail dimers, heterocycles with only hydrogen bond accepting capability to the hinge (i.e., interacting with the NH of Cys532) were evaluated. We hypothesized an effective alternative would demonstrate an approximately fivefold decrease in enzyme binding potency from the loss of one hydrogen bond,[11a] but that the significant hydrophobic contact to Trp531 should lead to compounds that exhibit therapeutically relevant activity. We therefore focused our efforts on compounds that retained a fused bicyclic template; selected examples are shown in Table 1.[14]

Compound **2** is a modest inhibitor that was reported in our earlier work[11] and utilizes the pyridine nitrogen as a simple acceptor for interaction at the hinge region. Quinoline **3** showed ca. 10-fold improvement in enzyme inhibition and a modest improvement in cellular activity due to enhanced interaction with the indole of Trp531. Incorporating heteroatoms into the second ring made a striking difference to activity depending on the substitution pattern. Compounds **4** and **5** were inactive most likely due to the repulsion between the newly introduced hydrogen bond acceptor and the carbonyl of Cys532. On the contrary, pyrrolo[3,2-*b*]pyridine **6**, was well tolerated and showed activity similar to **3**. Further improvement in pERK potency was observed when a nitrogen atom was introduced at the ring fusion. Pyrazolo[1,5-*a*]pyrimidine **7**, demonstrated similar binding activity, but exhibited encouraging improvement in cellular activity. Figure 1 illustrates the proposed binding mode of **7**. We hypothesized that further substitution at the 3-position of the pyrazolopyrimidine would be sterically prohibited, while the 2-position offered a clear route toward the exterior of the ATP cleft; this position became the focus of subsequent optimization.

Table 1
B-Raf activity of compounds **1–7**

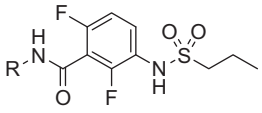

Compd	R	Braf IC_{50}[a] (nM)	pERK IC_{50}[a] (nM)
1	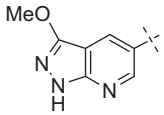	5	19
2		3880	6730
3	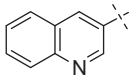	464	1381
4	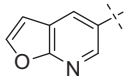	>10,000	–
5	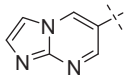	>10,000	–
6	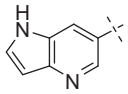	407	1513
7	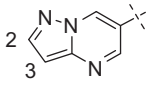	247	488

[a] IC_{50} values reflect the average from at least three separate experiments.

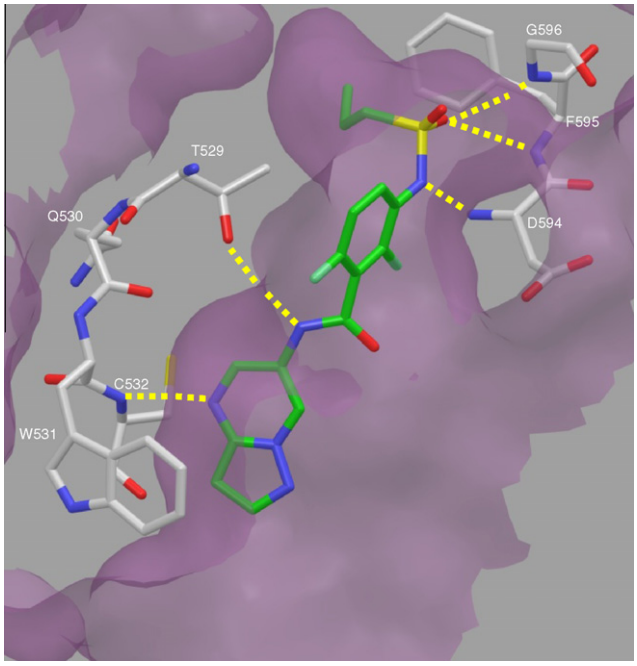

Figure 2. Proposed binding mode for compound **7**. The compound was modeled by analogy to a previously reported X-ray crystal structure of a pyrazolopyridine[11] followed by conformational minimization[15] The protein surface is rendered in violet, selected residues are depicted in white, and the inhibitor is green. Hydrogen bonds are illustrated as yellow dashed lines. The close contact between C3 of the pyrazolo[1,5-*a*]pyrimidine and the carbonyl of Cys532 is readily relieved by minor movement of the mainchain and the bicyclic template, with no disruption of other relevant interactions.

A number of alkyl and N-substituted pyrazolopyrimidines were synthesized and representative examples are shown in Table 2. Small alkyl groups, such as Me (**8**) and Et (**9**), gave a small twofold improvement in potency. No further improvement in activity was observed with a larger group (**11**). The potency of amino derivatives (**13**–**16**) was similar, generating compounds with pERK activities between 300–500 nM, regardless of their size. While smaller substituents were readily accommodated at the exit of the ATP cleft, they were of insufficient size to make additional contact; larger C2 substituents (i.e., **15–16**) appeared to be sterically demanding enough to cancel the potential for Van der Waals interactions.

Alkoxyl substituted pyrazolopyrimidines were prepared next and proved to be more potent (Table 3). The conjugated *O*-alkyl moiety resides near the exit of the ATP cleft and exerts a conformational control via repulsion between the oxygen and N1 σ lone pairs[16]; this orients the alkyl group toward a small depression near the main chain of Ser535 and Ser536 (Fig. 3). Methoxypyrazolopyrimidine **17**, with a pERK IC_{50} of 68 nM, is sevenfold more potent than the unsubstituted pyrazolopyrimidine **7**. The promising activity of **17** led us to further profile its physicochemical properties.

Table 2
B-Raf activity of alkyl and N-substituted pyrazolopyrimidines

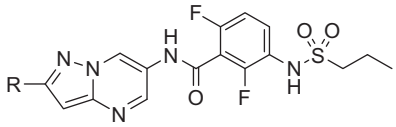

Compd	R	Braf IC_{50}[a] (nM)	pERK IC_{50}[a] (nM)
8	CH_3	131	248
9	CH_2CH_3	105	228
10	Cyclopropyl	124	299
11	Cyclopentyl	128	448
12	CF_3	126	374
13	$NHCH_3$	129	382
14	NH-*i*-Pr	190	395
15	Pyrrolidinyl-1-yl	367	664
16	Morpholino	174	315

[a] IC_{50} values reflect the average from at least three separate experiments.

Table 3
B-Raf activity of aryl/heteroaryl and O-substituted pyrazolopyrimidines

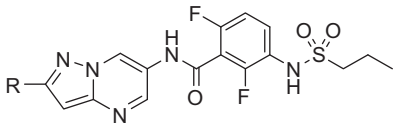

Compd	R	Braf IC_{50}[a] (nM)	pERK IC_{50}[a] (nM)
17	OMe	43	68
18	OEt	83	205
19	O-*i*-Pr	149	449
20	$O(CH_2)_2OMe$	67	110
21	Ph	7	17
22	3-F-Ph	19	60
23	4-F-Ph	11	54
24	3-pyridinyl	13	27
25	1-Me-pyrazolo-4-yl	13	48

[a] IC_{50} values reflect the average from at least three separate experiments.

Compared to **1**, crystalline **17** showed a 47 °C drop in melting point (182 °C vs 229 °C). This observation indicated a lower crystal packing energy associated with the pyrazolopyrimidine template. The decreased melting point coupled with a lower *C*log*P* (1.2) for **17** translated to a fivefold improvement in solubility (21 μg/mL at pH 6.5) over **1** (*C*log*P* = 1.6). Further elaboration of this series with larger alkoxy groups, for example OEt (**18**) and O-*i*-Pr (**19**), led to a decrease in activity. An extended alkoxy chain (**20**) restored some of the loss of potency.

Installation of aryl and heteroaryl groups resulted in the identification of several highly active B-Raf inhibitors (Table 3). These substituents make lipophilic contacts with several residues that form the exit from the ATP cleft (i.e., Ile463, Trp531, Ser535, Ser536). Compound **21**, a phenyl substituted pyrazolopyrimidine, was as potent as **1** with a pERK IC_{50} of 14 nM. Heteroaromatics, such as 3-pyridyl- (**24**) and 1-methylpyrazolo- (**25**) were also tolerated and similarly active. Due to its potent cellular activity, **21** was screened in a panel of 65 protein kinases at 1 μM and those with >30% inhibition are shown in Table 4. Overall, compound **21** exhibited excellent kinase selectivity toward non-Raf kinases, with the exception of SRMS. In comparison to **1**, compound **21** showed improved kinase selectivity against FGR and PTK6. Although compound **1** and **21** appear to be pan-Raf inhibitors, with similar activities towards B-Raf^{V600E}, B-Raf^{WT} and C-Raf^{WT}, both selectively inhibit the growth of B-Raf^{V600E} tumor lines. The ATP $K_{m(app)}$ for

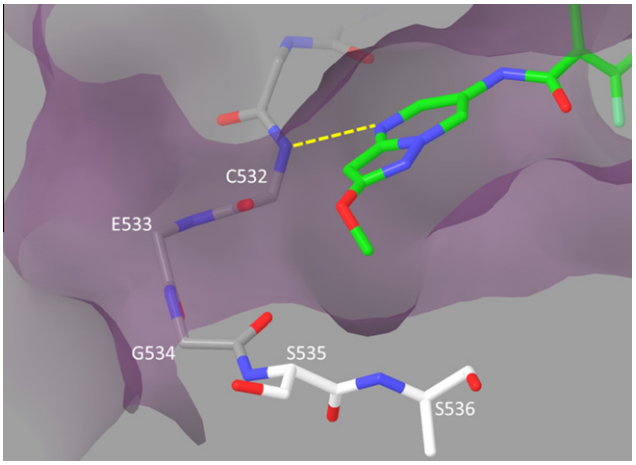

Figure 3. Proposed binding mode for compound **17**. The modeling and color scheme are as described for Figure 2. Sidechains for the hinge residues are undisplayed for clarity. The methoxy group is positioned for access to a small depression that exists near the mainchain atoms of residues Ser535 and Ser536.

Table 4
Kinase selectivity of compound **1** and **21**[a,b]

Compd	B-Raf^{V600E}	B-Raf^{WT}	C-Raf^{WT}	FGR	PTK6	SRMS
1	95	90	96	88	83	88
21	87	91	94	34	47	89

[a] Percent inhibition at 1 μM concentration of test compound.
[b] Value are means of at least two experiments.

B-Raf^{V600E} (65 μM) is notably higher than WT enzymes (ATP $K_{m(app)}$ 3–5 μM). This difference in affinity for ATP between the Raf isoforms results in the inhibitors functioning as comparatively weak Raf^{WT} inhibitors in cells, where ATP concentrations are at the mM concentration.[17]

The pyrazolo[1,5-*a*]pyrimidines were prepared according to Scheme 1.[18] Condensation of 3-substituted-5-aminopyrazoles **26** with sodium nitromalonaldehyde provided pyrazolopyrimidines with a range of substituents at the 2-position. Reduction of the nitro group was carried out by hydrogenation to afford amino pyrimidine **27**, which was coupled with benzoic acid **28** to furnish compounds **7**–**25**.

The in vitro ADME and physiochemical properties of **17** and **21** were determined (Table 5). Both compounds were found to be intrinsically stable in mouse microsomes with good permeability and displayed no inhibition of cytochrome P450 enzymes at 25 μM. While compound **17** exhibited improved aqueous solubility over **1**, compound **21** has virtually no solubility at neutral pH, as a

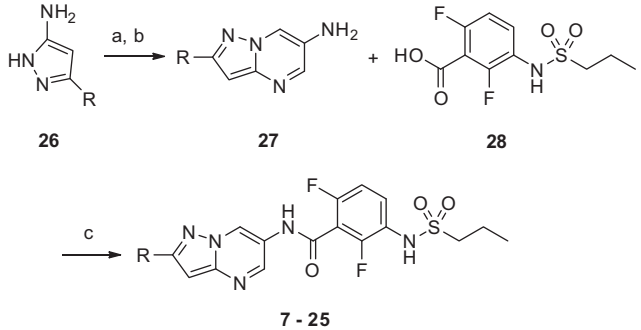

Scheme 1. Preparation of pyrazolo[1,5-*a*]pyrimidines: (a) sodium nitromalonaldehyde monohydrate, AcOH, 22-40 °C, 16 h; (b) H_2, 10% Pd/C, EtOH, 4 h; (c) EDCI, HOBt, DMF, 22 °C, 15 h.

Table 5
ADME properties of **17** and **21**

Compd	Clearance[a]	Caco-2[b]	CYP3A4 inhibition[c]	Sol. @ pH 6.5 and 7.4[d]
17	28	Medium	>25	21,32
21	10	High	>25	1,1

[a] Mouse microsome clearance (ml/min/kg).
[b] Caco-2-permeability classification: low ($<2 \times 10^{-6}$ cm/s), medium ($2–8 \times 10^{-6}$ cm/s), high ($>8 \times 10^{-6}$ cm/s).
[c] μM.
[d] μg/mL.

Table 6
Pharmacokinetic properties of **17** versus **1**

Compd	AUC[a]	CL[b]	%*F*	Vd[c]	Sol. @ pH 1.2, 6.5, 7.4[d]
17	733	1.0	98	0.16	18,21,32
1	426	1.3	48	0.11	3,4,9

[a] Mouse PO PK at 30 mg/kg (μM h).
[b] Mouse IV PK at 2.5 mg/kg (ml/min/kg).
[c] L/kg.
[d] μg/mL.

result of the negative impact of increased molecular weight and lipophilicity ($C\log P = 3.1$).

Based on optimal combination of activity and physiochemical properties, **17** was advanced into mouse pharmacokinetic studies (Table 6). Similar to **1**, **17** exhibited low clearance and low volume of distribution. However, an oral dose of 30 mg/kg (dosed as a solution in 40/10/50, by volume, in PEG400/EtOH/H_2O) delivered a ~2-fold increase in exposure and oral bioavailability (%*F*) in comparison to **1**.

Furthermore, while the oral exposure of **1** as a crystalline suspension in 1% methylcellulose/0.5% Tween 80 in water is fourfold lower compared to solution dosing (30 mg/kg in mice, AUC of 105 vs 426), the oral exposure of **17** was equivalent to solution dosing when dosed as a crystalline suspension in the same suspension formula (30 mg/kg in mice, AUC of 844 vs 733). These improvements can be attributed to the improved aqueous solubility of **17**.

In summary, we have utilized a pyrazolo[1,5-*a*]pyrimidine core to produce B-Raf inhibitors with excellent potency and selectivity profiles. Optimization led to the identification of compound **17**, a potent, selective and orally available B-Raf inhibitor with favorable physiochemical and pharmacokinetic properties. These improvements made it feasible to use crystalline suspensions for efficacy and safety evaluations without relying on enabling vehicles, such as amorphous spray-dried dispersion. Further progress on these inhibitors will be reported in due course.

Acknowledgments

The authors thank Susan Rhodes, Jennifer Otten and Ben Colsen for Caco-2, CYP P450 inhibition and solubility determinations. The authors also thank Dr. Steve Wenglowsky for critical review of the manuscript and helpful suggestions.

References and notes

1. Peyssonnaux, C.; Eychene, A. *Biol. Cell.* **2001**, *93*, 53.
2. Davies, H.; Bignell, G. R.; Cox, C.; Stephens, P.; Edkins, S.; Clegg, S.; Teague, J.; Woffendin, H.; Garnett, M. J.; Bottomley, W.; Davis, N.; Dicks, E.; Ewing, R.; Floyd, Y.; Gray, K.; Hall, S.; Hawes, R.; Hughes, J.; Kosmidou, V.; Menzies, A.; Mould, C.; Parker, A.; Stevens, C.; Watt, S.; Hooper, S.; Wilson, R.; Jayatilake, H.; Gusterson, B. A.; Cooper, C.; Shipley, J.; Hargrave, D.; Pritchard-Jones, K.; Maitland, N.; Chenevix-Trench, G.; Riggins, G. J.; Bigner, D. D.; Palmieri, G.; Cossu, A.; Flanagan, A.; Nicholson, A.; Ho, J. W. C.; Leung, S. Y.; Yuen, S. T.; Weber, B. L.; Seigler, H. F.; Darrow, T. L.; Paterson, H.; Marais, R.; Marshall, C. J.; Wooster, R.; Stratton, M. R.; Futreal, P. A. *Nature* **2002**, *417*, 949.
3. Pollock, P. M.; Harper, U. L.; Hansen, K. S.; Yudt, L. M.; Stark, M.; Robbins, C. M.; Moses, T. Y.; Hostetter, G.; Wagner, U.; Kakereka, J.; Salem, G.; Pohida, T.; Heenean, P.; Duray, P.; Kallioniemi, O.; Hayward, N. K.; Trent, J. M.; Meltzer, P. S. *Nat. Genet.* **2003**, *33*, 19.
4. (a) Gorden, A.; Osman, I.; Gai, W.; He, D.; Huang, W.; Davidson, A.; Houghton, A. N.; Busam, K.; Polsky, D. *Cancer Res.* **2003**, *63*, 3955; (b) Kuman, R.; Angelini, S.; Czene, K.; Sauroja, I.; Hahka-Kemppinen, M.; Pyrhonen, S.; Hemminki, K. *Clin. Cancer Res.* **2003**, *9*, 3362.
5. Wan, P. T.; Garnett, M. J.; Roe, S. M.; Lee, S.; Niculescu-Duvaz, D.; Good, V. M.; Jones, C. M.; Marshall, C. J.; Springer, C. J.; Barford, D.; Marais, R. *Cell* **2004**, *116*, 855.
6. (a) Samowitz, W. S.; Sweeney, C.; Herrick, J.; Albertsen, H.; Levin, T. R.; Murtaugh, M. A.; Wolff, R. K.; Slattery, M. L. *Cancer Res.* **2005**, *65*, 6063; (b) Riesco-Eizaguirre, G.; Gutiérrez-Martínez, P.; García-Cabezas, M. A.; Nistal, M.; Santisteban, P. *Endocr.-Relat Cancer* **2006**, *13*, 257; (c) Houben, R.; Becker, J. C.; Kappel, A.; Terheyden, P.; Bröcker, E. B.; Goetz, R.; Rapp, U. R. *J. Carcinog.* **2004**, *3*, 6.
7. Sawyers, C. *Nature* **2004**, *432*, 294.
8. Puzanov, I.; Flaherty, K. T.; Sosman, J. A.; Grippo, J. F.; Su, F.; Nolop, K.; Lee, R. J.; Bollag, G. *Drugs Future* **2011**, *36*, 191.
9. Exelixis has reported preliminary Phase 1 data on XL281: (a) Schwartz, G. L.; Roberson, S.; Shen, A.; Wang, E.; Pace, L.; Dials, H.; Mendelson, D.; Shannon, P.; Gordon, M. *J. Clin. Oncol.* **2009**, *27*, 3513. 15sAbstr; GSK has reported phase 1/2 data on dabrafenib, GSK2118436: (b) Kefford, R.; Arkenau, H.; Brown, M. P.; Millward, M.; Infante, J. R.; Long, G. V.; Ouellet, D.; Curtis, M.; Lebowitz, P. F.; Falchook, G. S. *J. Clin. Oncol.* **2010**, *28*, 8503. 15sAbstr.
10. (a) Takle, A. K.; Brown, M. J. B.; Davies, S.; Dean, D. K.; Francis, G.; Gaiba, A.; Hird, A. W.; King, F. D.; Lovell, P. J.; Naylor, A.; Reith, A. D.; Steadman, J. G.; Wilson, D. M. *Biorg. Med. Chem. Lett.* **2006**, *16*, 378; (b) Hansen, J. D.; Grina, J.; Newhouse, B.; Welch, M.; Topalow, G.; Littman, M.; Callego, M.; Gloor, G.; Martinson, M.; Laird, E.; Brandhuber, B. J.; Vigers, G.; Morales, T.; Woessner, R.; Randolph, N.; Lyssikatos, J.; Olivero, A. *Biorg. Med. Chem. Lett.* **2008**, *18*, 4692; (c) Tang, J.; Hamajima, T.; Nakano, M.; Sato, H.; Dickerson, S. H.; Lackey, K. E. *Biorg. Med. Chem. Lett.* **2008**, *18*, 4610; (d) Smith, A. L.; DeMorin, F. F.; Paras, M. A.; Huang, Q.; Petkus, J. K.; Doherty, E. M.; Nixey, T.; Kim, J. L.; Whittington, D. A.; Epstein, L. F.; Lee, M. R.; Rose, M. J.; Babij, C.; Fernando, M.; Hess, K.; Le, Q.; Beltran, P.; Carnahan, J. *J. Med. Chem.* **2009**, *52*, 6289.
11. (a) Wenglowsky, S.; Ren, L.; Ahrendt, K. A.; Laird, E. R.; Aliagas, I.; Alicke, B.; Buckmelter, A. J.; Choo, E. F.; Dinkel, V.; Feng, B.; Gloor, S. L.; Gould, S. E.; Gross, S.; Gunzner-Toste, J.; Hansen, J. D.; Hatzivassiliou, G.; Liu, B.; Malesky, K.; Mathieu, S.; Newhouse, B.; Raddatz, N. J.; Ran, Y.; Rana, S.; Randolph, N.; Risom, T.; Rudolph, J.; Savage, S.; Selby, L. T.; Shrag, M.; Song, K.; Sturgis, H. L.; Voegtli, W. C.; Wen, Z.; Willis, B. S.; Woessner, R. D.; Wu, W.-I.; Young, W. B.; Grina, J. *ACS Med. Chem. Lett.* **2011**, *2*, 342; (b) Wenglowsky, S.; Ahrendt, K. A.; Buckmelter, A. J.; Feng, B.; Gloor, S. L.; Gradl, S.; Grina, J.; Hansen, J. D.; Laird, E. R.; Lunghofer, P.; Mathieu, S.; Moreno, D.; Newhouse, B.; Ren, L.; Risom, T.; Rudolph, J.; Seo, J.; Sturgis, H. L.; Voegtli, W. C.; Wen, Z. *Biorg. Med. Chem. Lett.* **2011**, *21*, 5533.
12. Vasconcelos, T.; Sarmento, B.; Costa, P. *Drug Discovery Today* **2007**, *12*, 1068.
13. Wenglowsky, S.; Moreno, D.; Rudolph, J.; Ran, Y.; Ahrendt, K. A.; Arrigo, A.; Colsen, B.; Gloor, S. L.; Hasting, G. *Biorg. Med. Chem. Lett.* **2011**. doi:10.1016/j.bmcl.2011.12.030.
14. Inhibitor enzyme activity was determined utilizing full-length B-Raf^{V600E}. Inhibition of basal ERK phosphorylation in Malme-3 M cells was used as the mechanistic cellular assay.
15. The Maestro program was used to generate and manually position the structure into the X-ray coordinates of B-Raf in complex with a pyrazolopyridine analog,[11] followed by 500 steps of local minimization with the OPLS potential function. Maestro Version 9.0, Schrodinger, LLC; Portland OR.
16. The conformation constraining the lone pairs in a syn orientation resides 3.6 kcal/mol higher in energy than the anti, as computed using the 6-31G(d) basis set. GAMESS version 24: Schmidt, M. W.; Baldridge, K. K.; Boatz, J. A.; Elbert, S. T.; Gordon, M. S.; Jensen, J. H.; Koseki, S.; Matsunaga, N.; Nguyen, K. A.; Su, S. J.; Windus, T. L.; Dupuis, M.; Montgomery, J. A. *J. Comput. Chem.* **1993**, *14*, 1347.
17. Hatzivassiliou, G.; Song, K.; Yen, I.; Brandhuber, B. J.; Anderson, D. J.; Alvarado, R.; Ludlam, M. C.; Stokoe, D.; Gloor, S. L.; Vigers, G.; Morales, T.; Aliagas, I.; Liu, B.; Siberis, S.; Hoeflich, K. P.; Jaiswal, B. S.; Seshagiri, S.; Koeppen, H.; Belvin, M.; Friedman, L. S.; Malek, S. *Nature* **2010**, *464*, 431.
18. Gradl, S.; Rudolph, J.; Ren, L. WO 2011/025951.